structural feature of the site is the bridged binding of exogenous ligands between the type 2 and each of the type 3 coppers. It is now important to extend these studies in order to probe the interactions of exogenous ligands with the trinuclear site in partially reduced, catalytically relevant oxidation states and to directly characterize the structures of the bound oxygen intermediates in both native and T1Hg laccase.

Acknowledgment. We are grateful to the National Institutes of Health for support (Grant AM31450) P.A.C. acknowledges the National Institutes of Health for a postdoctoral fellowship (Grant GM13606). We thank Georgia Papaefthymiou for assistance with the SQUID magnetometer at MIT and Professor Christopher Reed and Robert Orosz for assistance with the magnetometer at U.S.C. We thank Dr. Peter Sandusky for assistance with the initial T1Hg experiments, Edward Yang for providing the met-T2D sample, and Professor Dean E. Wilcox for assistance in obtaining the met-T2D susceptibility data.

Registry No. Cu, 7440-50-8; laccase, 80498-15-3; azide, 14343-69-2.

Binuclear Electron Reservoir Complexes. Synthesis, Stabilization, and Electronic Structures of the 36- and 37-Electron Complexes $[\{Fe(C_5R_5)\}_2(\mu_2,\eta^n\text{-}C_{10}H_8)]^{m+}$ (R = H, Me): From Biphenyl (m = 1 and 2, n = 12) to Bicyclohexadienylidene (m = 0, n = 10)

Marc Lacoste,[†] Hassan Rabaâ,[‡] Didier Astruc,*[,†,⊥] Nicole Ardoin,[†] François Varret,[§] Jean-Yves Saillard,*[,‡] and Albert Le Beuze[‡]

Laboratoire de Chimie Organique et Organométallique, URA CNRS No. 35, 351 Cours de la Libération, 33405 Talence Cédex, France, Laboratoire de Chimie du Solide et Inorganique Moléculaire, Université de Rennes I, Campus de Beaulieu, 35042 Rennes Cédex, France, and Département de Recherches Physiques, URA CNRS No. 71, Université de Paris 6, 75252 Paris Cédex 05, France. *Received March 9, 1990*

Abstract: The reduction of $[(FeCp)_2(biphenyl)]^{2+}$ ($\mathbf{2a}^{2+}$) was found to be a chemically and electrochemically reversible two-electron process by cyclic voltammetry in DMF at −38 °C. With $LiAlH_4$ this 2e reduction in THF at −80 °C gives an ESR-silent blue species **2**, unstable above −50 °C, the structure of which was searched by using Cp* (Cp* = C_5Me_5). The 2e reduction of the new complex $[(FeCp^*)_2(biphenyl)]^{2+}(PF_6^-)_2$ ($\mathbf{2b}^{2+}$), using Na/Hg in THF at 20 °C gives the ESR-silent stable blue diamagnetic complex **2b**, analogous to **2a**, whereas the cyclic voltammogram of $\mathbf{2b}^{2+}$ shows close reversible one-electron waves. The complex **2b** was shown by ^1H and ^{13}C NMR and Mössbauer spectroscopy to have a 36e Fe_2^{II}bicyclohexadienylidene structure. Comproportionation (K = 172 at 20 °C) was achieved by mixing $\mathbf{2b}^{2+}(PF_6^-)_2$ and **2b** in THF at 20 °C, which gives an 80% yield of the green mixed-valence complex $\mathbf{2b}^+$. The latter is a 37e complex with a weak distortion of the biphenyl ligand and showed 3g values in ESR characterizing a Fe^IFe^{II} complex. Its Mössbauer spectra at 0 field are essentially temperature independent and only contain one quadrupole doublet between 4 and 293 K with an isomer shift and a quadrupole splitting intermediate between those of Fe^I and Fe^{II} monomeric units. This indicates an average valence structure with delocalization or fast electron hopping. Under a field of 6 T, an isotropic value of −3.3 T is obtained for the saturation hyperfine tensor [**A**]. For the latter, an expected orbital contribution of −0.4 T, mainly representing the contact term, corresponds to 25% of the total spin density on the biphenyl ligand of $\mathbf{2b}^+$. SCF–MS–Xα calculations on $\mathbf{2a}^{2+}$, $\mathbf{2a}^+$, and **2a** show that, when $\mathbf{2a}^{2+}$ is reduced, the first electron transfer involves a metallic b_u level, which has some π_{CC} antibonding character between the two atoms linking the phenyl rings. The second electron transfer is accompanied by a significant increase of this π_{CC} antibonding character. A decreasing of the π_{CC} bonding character of the highest occupied levels of a_g symmetry is also noted. Additional calculations on $\mathbf{1a}^{2+}$ [Fe_2-(μ^2,η^{12}-fulvalene)(biphenyl)]$^{2+}$ ($\mathbf{1a}^{2+}$) (isomer of $\mathbf{2a}^{2+}$) indicate that, in contrast to the unoccupied b_u biphenylic level of $\mathbf{2a}^{2+}$, the corresponding fulvenic b_u level is too high in energy to be accessible. Consistently, the reduction of $\mathbf{1a}^{2+}$ is essentially a metal reduction, whereas the reduction of $\mathbf{2a}^{2+}$ can be considered as only involving the biphenyl ligand. Altogether, an accurate determination of the electronic and structural transformation (including their orbital description and thermodynamic estimation) that occurs upon each ET of a fast, reversible 2e-transfer process is reported for the first time, which allows for understanding and thus designing of fast 2e-transfer reagents.

Introduction

The investigations of the electronic structure of mixed-valence bi-[1] and polynuclear[2] inorganic complexes have provided much insight regarding intramolecular electron and charge transfer or delocalization.[1-3] Organic ligands such as fulvalene in biferrocene[4,5] also bring about analogous problems of localization vs delocalization of the mixed valence.[5] The information gained from these studies is of potential use in applied areas such as solar energy storage,[6] where intramolecular electron transfer is a key step. Hendrickson has shown that the lattice, i.e., the counteranion,

[†] Laboratoire de Chimie Organique et Organométallique.
[‡] Laboratoire de Chimie du Solide et Inorganique Moléculaire.
[§] Département de Recherches Physiques.
[⊥] Present address (until September 30, 1991): Department of Chemistry, University of California, Berkeley, CA 94720.

(1) (a) Holm, R. H. In *Biological Aspects of Inorganic Chemistry*, Addison, A. W.; Cullen, W. R.; Dolphin, D.; James, B. R., Eds.; Wiley: New York, 1977; Chapter 2. Nherland, S.; Gray, H. B. *Ibid.* Chapter 10. (b) Trinh-Toan; Teo, B. K.; Ferguson, J. A.; Meyer, T. J.; Dahl, L. F. *J. Am. Chem. Soc.* **1977**, *99*, 408. (c) Wiegardt, K.; Bossek, U.; Nuber, B.; Wiess, J.; Bonvoisin, J.; Corbella, M.; Vitols, S. E.; Girerd, J.-J. *J. Am. Chem. Soc.* **1988**, *110*, 7398. (d) Connelly, N. G.; Geiger, W. E. *Adv. Organomet. Chem.* **1984**, *23*, 1. (e) Eisenbroich, C.; Heck, J.; Massa, W.; Nun, E.; Schmitt, R. *J. Am. Chem. Soc.* **1983**, *105*, 2905. (f) Sharp, P. R.; Raymond, K. N.; Smart, J. C.; McKinney, R. J. *J. Am. Chem. Soc.* **1981**, *103*, 753.
(2) (a) Geiger, W. E.; Connelly, N. G. *Adv. Organomet. Chem.* **1985**, *24*, 87. (b) Chu, T. T.-H.; Lo, F. Y.-K.; Dahl, L. F. *J. Am. Chem. Soc.* **1982**, *104*, 3409. (c) Ferguson, J. A.; Meyer, T. J. *J. Chem. Soc., Chem. Commun.* **1971**, 623. (d) Kubas, G. J.; Vergamini, P. *Inorg. Chem.* **1981**, *20*, 2667.

0002-7863/90/1512-9548$02.50/0

Scheme I: Comparison of the Fulvalene-Bridged Series 1^{2+} with the Biphenyl-Linked Series 2^{2+} [a]

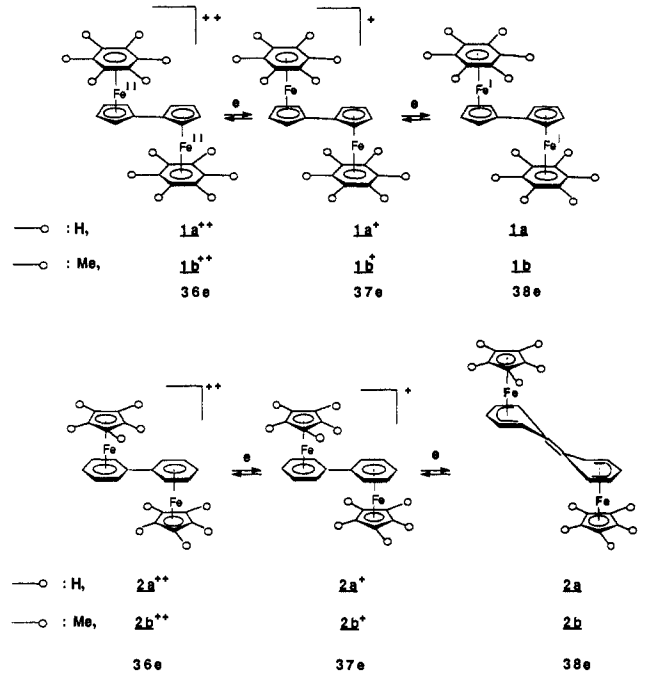

[a] No major structural changes along the reduction $1^{2+} \rightarrow 1$. Note the structural change in **2**. In the fulvalene series **1**, for which no structural change occurs upon at least two 1e reductions, the cyclic voltammogram (Hg, DMF) showed four waves separated by 0.3–0.5 V.[9b]

greatly influences the localization of the mixed valence in 35e biferrocene cation and its alkyl derivatives.[5] It has been indicated that the molecular electronic structure and the lattice are strongly coupled in Fe^{I} sandwiches via the cooperative dynamic Jahn–Teller effect as monitored by Mössbauer spectroscopy.[7-10] In addressing the studies of binuclear radicals, we have varied the nature of the bridging organic ligand. Fulvalene vs biphenyl has been used to link both iron centers (Scheme I), allowing the modulation of the set of HOMOs and LUMOs.

Since the LUMO of the fulvalene series has a much higher energy than that of the biphenyl series, the former does not lead to reduction of the ligand (intramolecular coupling) whereas the latter does. This rationalization stems from the theoretical calculations and compares with the experimental data, which are detailed in this article. The fulvalene series is not subjected to significant structural reorganization upon two or three successive reversible monoelectronic transfers. On the other hand, the biphenyl series gives rise to intramolecular coupling upon transfer of two electrons, characterized by a structural reorganization recorded by X-ray spectroscopy. The reduced biphenyl ligand is thus transformed into a bicyclohexadienylidene η^5 bonded to each iron atom in a ferrocene-like 18e configuration. Some synthetic and structural results have been reported in their preliminary form.[10a,b] In this paper, we are reporting in detail the synthetic, electrochemical, electronic structure, and theoretical ($X\alpha$) data on the novel family of complexes $[\{Fe(C_5Me_5)\}_2(biphenyl)]^{n+}$, $\mathbf{2b}^{n+}$, including the Cp*-stabilized three oxidation states $n = 0$–2. The new mixed-valence 37 electron complex $\mathbf{2b}^{+}$ ($n = 1$) is subjected to an accurate spectroscopic and theoretical scrutiny. We start by disclosing the two-electron reversible reduction of the parent complex $[(FeCp)_2(biphenyl)]^{2+}(PF_6^-)_2$ ($\mathbf{2a}^{2+}$). Then we use the accurate information on the permethylated series $\mathbf{2b}^{n+}$ and the comparison with the isomer $[Fe_2(fulvalene)(C_6H_6)]^{2+}$ ($\mathbf{1a}^{2+}$). This understanding should show how and why a fast two-electron transfer occurs in $\mathbf{2a}^{2+}$ and should find future use in the design of multielectronic redox catalysts required in energy conversion processes.[11]

Results

Syntheses of the Precursor Dicationic Complexes $[\{Fe(C_5R_5)\}_2(biphenyl)]^{2+}(PF_6^-)_2$ (R = H ($\mathbf{2a}^{2+}$); CH_3 ($\mathbf{2b}^{2+}$)). The parent precursor 36e complex $[(FeCp)_2(biphenyl)]^{2+}$ ($\mathbf{2a}^{2+}$) has been synthesized by Hendrickson et al.[12a,b] We have improved this synthesis by ligand exchange between ferrocene and biphenyl in the melt at 120 °C. The yield reaches 53% (eq 1).

We have already used $FeCp^*(CO)_2Br/AlCl_3$ to complex the $FeCp^*$ moiety to mononuclear aromatics.[7c,f] Extension of this principle now allows us to synthesize binuclear complexes of polyaromatics. As for the complexation of FeCp, the reactions give the best yields when they are carried out in the melt (eq 2).

(3) (a) Allen, G. C.; Hush, N. S. *Prog. Inorg. Chem.* **1967**, *8*, 357. (b) Robin, M. B.; Day, P. *Adv. Inorg. Chem. Radiochem.* **1976**, *10*, 227. (c) Taube, H. *Pure Appl. Chem.* **1975**, *44*, 25. (d) Brown, D. B. *Mixed Valence Compounds*, D. Reidel: Dordrecht, Holland, 1980.

(4) (a) Morrison, W. H.; Hendrickson, D. N. *J. Chem. Phys.* **1973**, *59*, 380. (b) Cowan, D. O.; Collins, R. L.; Kaufman, F. *J. Chem. Phys.* **1971**, *75*, 2025. (c) Morrison, W. H.; Krogsud, S.; Hendrickson, D. N. *Inorg. Chem.* **1973**, *12*, 1998. (d) Collins, R. L.; Candela, G. A.; Kaufman, F. *J. Am. Chem. Soc.* **1971**, *93*, 3889. (e) Kaufman, F.; Cowan, D. O. *J. Am. Chem. Soc.* **1970**, *92*, 6198. (f) Cowan, D. O.; Park, J.; Barber, M.; Swift, P. *J. Chem. Soc., Chem. Commun.* **1971**, 1444. (g) Cowan, D. O.; Levanda, C.; Park, J.; Kaufman, F. *Acc. Chem. Res.* **1973**, *6*, 1. (h) Rudie, A. W.; Davison, A.; Frankel, R. B. *J. Am. Chem. Soc.* **1979**, *101*, 1629. (i) Morrison, W. H.; Hendrickson, D. N. *Inorg. Chem.* **1975**, *14*, 2331. (j) Iijima, S.; Saida, R.; Motoyama, I.; Sano, H. *Bull. Chem. Soc. Jpn.* **1981**, *54*, 1375. (k) Motoyama, I.; Suto, K.; Katada, M.; Sano, H. *Chem. Lett.* **1983**, 1215.

(5) (a) Hendrickson, D. N.; Oh, S. M.; Moore, M. F. *Comments Inorg. Chem.*, 1985, *4*, 329, and references therein. (b) Dong, T. Y.; Hendrickson, D. N.; Pierpont, C. G.; Moore, M. F. *J. Am. Chem. Soc.* **1986**, *108*, 4423. (c) Dong, T. Y.; Kambara, T.; Hendrickson, D. N. *J. Am. Chem. Soc.* **1986**, *108*, 963. (d) Dong, T. Y.; Hendrickson, D. N.; Iwai, K.; Cohn, M. J.; Geib, S. J.; Rheingold, A. L.; Sano, H.; Motoyama, I.; Nakashima, S. *J. Am. Chem. Soc.* **1985**, *107*, 7996. (e) Webb, R. J.; Geib, S. J.; Staley, D. L.; Rheingold, A. L.; Hendrickson, D. N. *J. Am. Chem. Soc.* **1990**, *112*, 5031.

(6) For an excellent and extensive review of biferrocene and difulvalene diiron systems and their use in the catalysis of H_2 formation from acids, see: Mueller-Westerhoff, U. T. *Angew. Chem., Int. Ed. Engl.* **1986**, *25*, 702 (review).

(7) (a) Astruc, D.; Hamon, J.-R.; Althoff, G.; Román, E.; Batail, P.; Michaud, P.; Mariot, J.-P.; Varret, F.; Cozak, D. *J. Am. Chem. Soc.* **1979**, *101*, 5445. (b) Mariot, J.-P.; Astruc, D.; Batail, P.; Varret, F. *J. Phys.* **1980**, *1*, 319. (c) Hamon, J.-R.; Astruc, D.; Michaud, P. *J. Am. Chem. Soc.* **1980**, *103*, 758. (d) Astruc, D.; Hamon, J.-R.; Román, E.; Michaud, P. *J. Am. Chem. Soc.* **1980**, *103*, 7502. (e) Mariot, J.-P.; Michaud, P.; Lauer, S.; Astruc, D.; Trautwein, A. X.; Varret, F. *J. Phys.* **1983**, *44*, 1377. (f) Astruc, D. *Tetrahedron* **1983**, *39*, 4027 (Report 157). (g) Guerchais, V.; Astruc, D. *J. Chem. Soc., Chem. Commun.* **1984**, 881. (h) Hamon, J.-R.; Astruc, D.; Román, E.; Batail, P.; Mayerle, J. J. *J. Am. Chem. Soc.* **1981**, *103*, 2431. (i) Michaud, P.; Astruc, D.; Ammeter, J. H. *J. Am. Chem. Soc.* **1982**, *104*, 3755.

(8) (a) Rajasekharan, M. V.; Giezynski, S.; Ammeter, J. H.; Ostwald, N.; Hamon, J.-R.; Michaud, P.; Astruc, D. *J. Am. Chem. Soc.* **1982**, *104*, 2400. (b) Catheline, D.; Astruc, D. *J. Organomet. Chem.* **1982**, *226*, C52. (c) Michaud, P.; Mariot, J.-P.; Varret, F.; Astruc, D. *J. Chem. Soc., Chem. Commun.* **1982**, 1383. (d) Green, J. C.; Kelly, M. R.; Payne, M. P.; Seddon, E. A.; Astruc, D.; Hamon, J.-R. *Organometallics* **1983**, *2*, 211. (e) Astruc, D. *Acc. Chem. Res.* **1986**, *19*, 377. (f) Lacoste, M.; Desbois, M.-H.; Astruc, D. *Nouv. J. Chim.* **1987**, 561. (g) Astruc, D. *Chem. Rev.* **1988**, *88*, 1189. (h) Madonik, A.; Astruc, D. *J. Am. Chem. Soc.* **1984**, *106*, 2437.

(9) (a) Desbois, M.-H.; Astruc, D.; Guillin, J.; Mariot, J.-P.; Varret, F. *J. Am. Chem. Soc.* **1985**, *107*, 52. (b) Desbois, M.-H.; Astruc, D. *Organometallics* **1989**, *8*, 1841. (c) Desbois, M.-H.; Astruc, D.; Guillin, J.; Varret, F. *Organometallics* **1989**, *8*, 1848. (d) Desbois, M.-H.; Astruc, D.; Guillin, J.; Varret, F.; Trautwein, A. X. *J. Am. Chem. Soc.* **1989**, *111*, 5800.

(10) (a) Lacoste, M.; Varret, F.; Toupet, L.; Astruc, D. *J. Am. Chem. Soc.* **1987**, *109*, 6504. (b) Astruc, D.; Lacoste, M.; Toupet, L. *J. Chem. Soc., Chem. Commun.* **1990**, 558. (c) Lacoste, M.; Astruc, D. *J. Chem. Soc., Chem. Commun.* **1987**, 667. (d) Lacoste, M.; Rabaa, H.; Astruc, D.; Le Beuze, A.; Saillard, J.-Y.; Précigoux, C.; Courseille, C.; Ardoin, N.; Bowyer, W. J. *Organometallics* **1989**, *8*, 2233.

(11) (a) Kalyanasundaran, K.; Grätzel, M.; Pelizetti, E. *Coord. Chem. Rev.* **1986**, *69*, 57. (b) Collman, J.-P.; Kim, K. *J. Am. Chem. Soc.* **1986**, *108*, 7847. (c) Hawecker, J.; Lehn, J.-M.; Ziessel, R. *Nouv. J. Chim.* **1983**, *7*, 271. (d) Wrighton, M. S. *Comments Inorg. Chem.* **1985**, *4*, 269.

(12) (a) Morrison, W. H.; Ho, E. Y.; Hendrickson, D. N. *Inorg. Chem.* **1975**, *14*, 500. (b) Morrison, W. H.; Ho, E. Y.; Hendrickson, D. N. *J. Am. Chem. Soc.* **1974**, *96*, 3603. (c) Nesmeyanov, A. N.; Vol'kenau, N. A.; Bolesova, I. N. *Dokl. Acad. Nauk. SSSR* **1966**, *166*, 607. (d) Nesmeyanov, A. N.; Denisovitch, L. I.; Gubin, S. P.; Vol'kenau, N. A.; Sirotkina, F. I.; Bolesova, I. N. *J. Organomet. Chem.* **1969**, *20*, 169. (e) Green, M. L. H.; Pratt, L.; Wilkinson, G. *J. Chem. Soc.* **1960**, 989. Khand, I. V.; Pauson, P. L.; Watts, W. E. *J. Chem. Soc. C* **1969**, 2024.

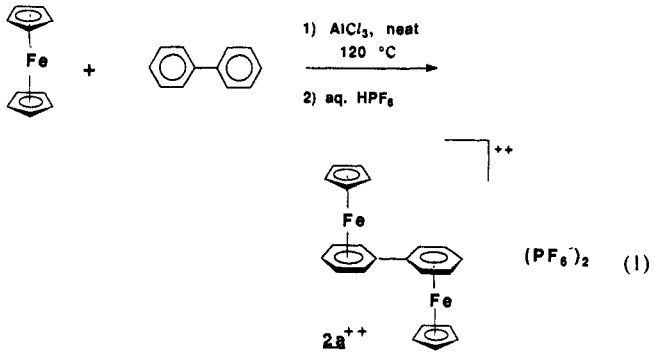

(1)

Recrystallization from acetonitrile gave a 32% yield of yellow crystals of $\mathbf{2b}^{2+}$ as the PF_6^- salt.

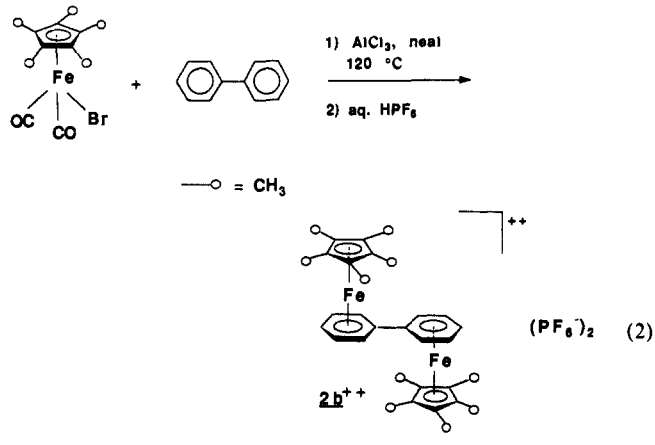

(2)

The structure and purity of $\mathbf{2b}^{2+}$ are shown by elemental analysis and ^1H and ^{13}C NMR. The multiplets of the biphenyl ligand appear between 6.1 and 6.2 ppm (^1H) whereas the substituted (δ 95.7 ppm), ortho (85.8 ppm), meta (91.5 ppm), and para (92.6 ppm) carbons are distinguished in the ^{13}C spectra.

Electrochemistry of [{Fe(C_5R_5)}$_2$(biphenyl)]$^{2+}$(PF_6^-)$_2$ (2^{2+}). (a) Cp Series: $\mathbf{2a}^{2+}$. The outstanding feature disclosed in the voltammogram of $\mathbf{2a}^{2+}$ is the single reversible wave found at −38 °C (DMF, *n*-Bu_4NBF_4 (0.1 M), Hg cathode) at $E°$ = 1.12 V vs SCE using ferrocene as the internal standard. The comparison of the height of the peak of $\mathbf{2a}^{2+}$ with those of ferrocene and biferrocene led to the finding that the wave of $\mathbf{2a}^{2+}$ is a two-electron wave. After the diffusion control was checked, the measurement of the ratio i_a/i_c = 1 showed chemical reversibility. The ΔE_p value is 28 mV, independent of scan rate, which indicated electrochemical reversibility and confirmed that this wave involves two electrons.

We were intrigued by the pioneering report from Hendrickson et al.[12a] on the polarography of $\mathbf{2a}^{2+}$ at 20 °C giving two waves at "$E_{1/2}$" = −1.17 and −1.32 V vs SCE and attributed to two successive one-electron transfers $\mathbf{2a}^{2+} \rightarrow \mathbf{2a}^{+} \rightarrow \mathbf{2a}$ including the mixed-valence $\mathbf{2a}^{+}$. Using cyclic voltammetry, we were able to confirm Hendrickson's experimental findings of two waves at 22 °C. However, the cyclic voltammogram (CV) shows that the chemical reversibility is nil for the first wave. The CVs at various temperatures between −38 and +22 °C were thus recorded and are compared in Figure 1. Since the first wave is not reversible in the room-temperature CV, we suspected the fast decomplexation of one iron–Cp moiety (ĒC process). We synthesized the monometallic complex [FeCp(biphenyl)]$^+PF_6^-$ ($\mathbf{3a}^+$),[7b,d,12c] in order to compare its CV[11b,d,12d] with that of the second wave of $\mathbf{2a}^{2+}$ at 22 °C. We indeed found that the second wave of $\mathbf{2a}^{2+}$ at 22 °C is due to the one-electron reduction of $\mathbf{3}^+$. This was shown by the independent recording of the CV of $\mathbf{3a}^+$ as well as by the increase of the second wave without potential shift upon recording the CV of $\mathbf{2a}^{2+}$ to which increasing amounts of $\mathbf{3a}^+$ had been added. From these experiments, it is now possible to conclude that the two waves of the CV of $\mathbf{2a}^{2+}$ at 22 °C are due to an ĒC process of **2a** (C = semidemetalation) followed by a reversible one-electron reduction of the monometallic complex [FeCp(biphenyl)]$^+PF_6^-$ (rather than to two successive one-electron reductions of $\mathbf{2a}^{2+}$ with a thermodynamically stable mixed-valence complex $\mathbf{2a}^+$).[12a]

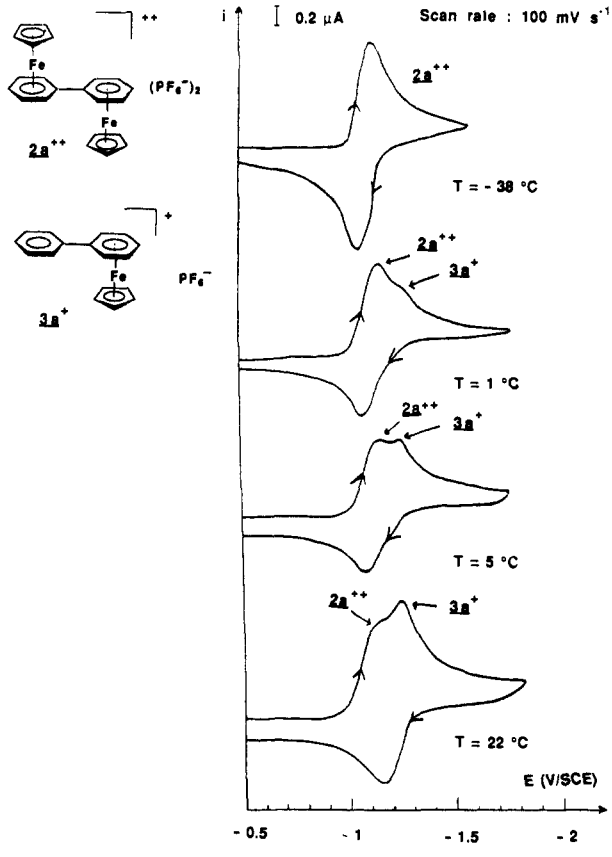

Figure 1. Cyclic voltammogram of $\mathbf{2a}^{2+}$ (DMF, *n*-Bu_4NBF_4 (0.1 M), Hg) at various temperatures showing the progressive formation of $\mathbf{3a}^+$, an ĒC process of $\mathbf{2a}^{2+}$, C being the loss of one FeCp moiety from $\mathbf{2a}^{2+}$. Note the increase of the wave of the monometal complex +3a^+, formed by the ĒC process (semidemetalation of **2**).

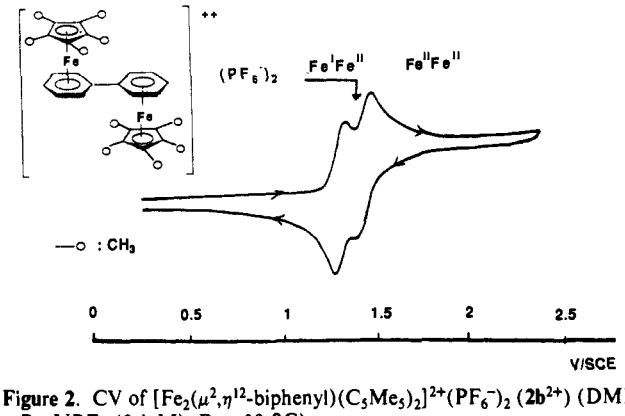

Figure 2. CV of [$Fe_2(\mu^2,\eta^{12}$-biphenyl)(C_5Me_5)$_2$]$^{2+}$(PF_6^-)$_2$ ($\mathbf{2b}^{2+}$) (DMF, *n*-Bu_4NBF_4 (0.1 M), Pt, −30 °C).

We also synthesized [$(FeCp)_2$(*p*,*p*′-dimethylbiphenyl)]$^{2+}$(PF_6^-)$_2$ ($\mathbf{2c}^{2+}$) and recorded its CV at −38 °C, which showed a chemically reversible wave (i_a/i_c = 1). However, the half-height width is slightly larger than that of $\mathbf{2a}^{2+}$. This can tentatively be attributed to the slight splitting of the two-electron wave into two very close one-electron waves (the second reduction would then be slightly more negative than the first one, contrary to the case of $\mathbf{2a}^{2+}$). Consistently, we also noted a larger ΔE_p (94 mV) than for $\mathbf{2a}^{2+}$. Again, this is consistent with the slight splitting of the two waves rather than with a slow electron transfer (quasi-reversibility).

(b) C_5Me_5 Series: $\mathbf{2b}^{2+}$. This phenomenon of the splitting of the two-electron wave of $\mathbf{2a}^{2+}$ into two close one-electron waves is clearly seen upon switching from the Cp to the C_5Me_5 series.

The CVs of [$Fe_2(\mu^2,\eta^{12}$-biphenyl)(C_5Me_5)$_2$]$^{2+}$(PF_6^-)$_2$ ($\mathbf{2b}^{2+}$) present two reduction waves at $E°$ = −1.27 and −1.4 V on the Pt

Table I. CVs Recorded at −35 °C on Hg Cathode (0.1 M n-Bu_4NBF_4, DMF)[a]

compound	first wave			second wave			
	$E°_1$	i_a/i_c	ΔE_p, mV	$E°_2$	i_a/i_c	ΔE_p, mV	$\Delta E°$
$[Fe_2Fv(C_6H_6)_2]^{2+}$	−1.15	1	60 (1e)	−1.47	1	70	0.320
$[Fe_2(diphenyl)Cp_2]^{2+}$	−1.12	1	28 (2e)				0
$[Fe_2(diphenyl)Cp^*_2]^{2+}$	−1.27	1	50 (1e)	−1.40	1	60	0.130
$[Fe_2(p,p'$-dimethyldiphenyl)$Cp_2]^{2+}$	−1.20	1	94 (2e)				
$[Fe_2(p,p'$-dimethyldiphenyl)$Cp^*_2]^{2+}$	−1.30	1	70 (1e)	−1.45	1	80	0.150

[a] $E°$ values in volts vs SCE, independent of the sweep rate. Data for $[Fe_2Fv(C_6H_6)]^{2+}$ are taken from ref 9a.

Table II. Compared ^{13}C Chemical Shifts for the Decoordinated Carbon of the Exocyclic Double Bond in Various Cyclohexadienyl and Cyclohexadienylidene Ligands

compounds	^{13}C for C= of the ring	ref
$[FeCp\{\eta^5\text{-}C_6Me_5(=CH_2)\}]$	140	7d
$[Fe(HMB)\{\eta^4\text{-}C_6Me_4(=CH_2)_2\}]$	144.8	8h
$[Cr_2(\eta^{10}$-biphenyl$)(CO)_6]^{2-}$	102.17	17
$[Fe_2Cp^*_2(\eta^{10}$-biphenyl$)]$	102.17	10a

cathode, which are both chemically and electrochemically reversible (i_a/i_c is a constant under diffusion control conditions; no variation of E_p's with scan rate, ΔE_p = 50 mV for the first wave and 60 mV for the second wave). No further reduction is observed to −3 V vs SCE. This trend is observed at 20 °C as well as at −35 °C and does not vary from the Pt to Hg cathode. With the height of the oxidation wave of ferrocene as a reference, both waves are found to involve one electron each. The CV data are summarized in Table I.

The observation of the stabilization of the mixed-valence complex in the CVs and of that of the 2e-reduced neutral complex led to the idea that the mixed-valence complex might be isolable in this case. The comproportionation constant derives from the $\Delta E°$ values (differences between the two thermodynamic potentials).[23]

$$[Fe_2(biphenyl)Cp^*_2]^{2+} + Fe_2(biphenyl)Cp^*_2 \rightleftarrows 2[Fe_2(biphenyl)Cp^*_2]^{+} \quad (3)$$

$$K = \theta^{\Delta E° F/RT}$$

where F is the Faraday constant (9.648 46 × 10^4 C/equiv), R is the molar gas constant (8.31441 J mol^{-1} K^{-1}), and T is temperature in kelvin ($\Delta E°$ in volts). Then K = 172 (20 °C).

The CV of the complex $[(FeCp^*)_2(p\text{-}CH_3\text{-biphenyl})^{2+}(PF_6^-)_2$ ($\mathbf{2d}^{2+}$) shows very similar trends. The two one-electron waves are now found at $E°$ = −1.30 and −1.45 V vs SCE under the same conditions (Table I). The potential difference between these two waves is slightly larger than for the biphenyl complex. This indicates that the second reduction is comparably more difficult, giving some more credit to our observation that this might also be the case of the Cp series (vide infra).

Two-Electron Reduction Using Redox Reagents: Bicyclohexadienylidene Complexes. The $LiAlH_4$ reduction of $\mathbf{2a}^{2+}$ in THF at −80 °C immediately gives an intense blue complex. Attempts to record an ESR spectrum of this complex under various conditions gave no ESR signal. This complex is very unstable and decomposes above −50 °C. We know that the low-temperature $LiAlH_4$ reduction of complexes of the $FeCp(arene)^+$ type gives electron transfer (ET) to generate the neutral Fe^I complex.[7i] It is also well-known that room-temperature hydride reduction of $FeCp(arene)^+$ complexes gives ferrocene-like orange $FeCp(\eta^5$-cyclohexadienyl) complexes.[12e] When the $LiAlH_4$ reduction of the precursor $FeCp(arene)^+$ cation is effected at low temperature (typically −80 °C) followed by warmup, the overall result is the same (hydride transfer), but it is decomposed in an ET at low temperature to form forest green Fe^I followed by H-atom transfer at higher temprature (−50 to 0 °C).[7i] Thus, we thought that the Fe^IFe^{II} or Fe^IFe^I proposed by Hendrickson upon electrochemical reduction of $\mathbf{2a}^{2+}$[12a] could be characterized at least by ESR subsequent to $LiAlH_4$ reduction of $\mathbf{2a}^{2+}$. Since this was not the case and since the blue color obtained detracted from the expected green color of Fe^I and Fe^IFe^I complexes, we reasoned that "abnormal" trends should be further sought by tentative reproduction of this chemistry using the stabilizing Cp* ligand.

Table III. Mössbauer parameters at 0 field and 77 K for CpFe(cyclohexadienyl)-type Complexes

77 K	IS (vs Fe)	QS
$[Fe(\eta^5\text{-}C_5H_5)(\eta^5\text{-}C_6Me_6H)$[7i]	0.43	1.88
$[Fe(\eta^5\text{-}C_5H_5)\{\eta^5\text{-}C_6Me_5(=CH_2)\}]$[7d]	0.43	1.88
$[Fe(\eta^5\text{-}C_5Me_5)_2$(bicyclohexadienylidene)] (*2b*)	0.564 (1)	1.653 (3)

[a] IS, isomer shift (mm/s); QS, quadrupole splitting (mm/s).

The Na/Hg reduction of $\mathbf{2b}^{2+}$ in THF at 20 °C is achieved in 3 h and gives a blue solution showing no sign of decomposition at 20 °C. Workup and recrystallization from toluene/pentane at −90 °C gave dark blue crystals of the neutral complex **2b** in 64% yield, which are air-sensitive but thermally stable (eq 4).

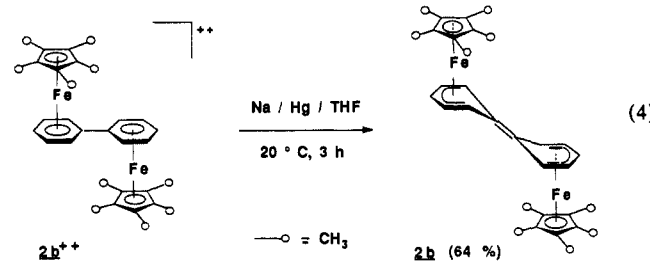

(4)

The ^1H and ^{13}C NMR spectra in C_6D_6 show that the neutral complex is diamagnetic and that the biphenyl ligand has been reduced to bicyclohexadienylidene: the para proton resonates at δ 5.6 ppm whereas the meta protons are found at δ 4.1 ppm and the ortho protons at δ 2.6 ppm. Similarly, the ^{13}C spectrum shows the bicyclohexadienylidene carbons at δ 77.7 ppm (para), δ 81.9 ppm (meta), δ 53.1 ppm (ortho), and δ 102.7 ppm (C=C). These ^1H and ^{13}C chemical shifts are characteristic of a cyclohexadienyl ligand. The ^{13}C shift of the decoordinated carbon is analogous to the one found recently for $[Cr(CO)_3]_2$(bicyclohexadienylidene)$]^{2-}$ (δ 102.17 ppm) and is 40 ppm lower than for a cyclohexadienyl carbon bound to an exocyclic methylene (Table II).

Thus, the electronic structure of **2b** corresponds to a ferrocene-like composition in which all the ligands are bound in a η^5 fashion to the Fe^{II} centers. The diamagnetism, the Fe^{II} oxidation state, and the analogy with $Fe^{II}Cp$(cyclohexadienyl)-type complexes is confirmed by the Mössbauer spectra of **2b** at zero field and by the data under a magnetic field of 6 T, which do now show a hyperfine field (Table III). Under 6 T, the low-asymmetry parameter (η = 0.9 close to the maximum value 1) indicates a modified sandwich structure with low symmetry as expected in the case of cyclohexadienyl complexes.

The X-ray crystal structure of **2b** (Figure 3a), which has been reported in the preliminary communication,[10a] confirms the existence of a bicyclohexadienylidene ligand coordinated in a η^5 fashion to both iron atoms. Its main features are an exocyclic full double bond (C_{11}–$C_{11'}$ = 1.37 Å) and a folding angle of 25° for the cyclohexadienyl ligands (angle between the mean C_{12}–C_{16} and the C_{11}–C_{12}–C_{16} planes). The value compares well with the folding angle of 32° reported for $[FeCp\{\eta^5\text{-}C_6Me_5(CH_2)\}]$.[7h] The distortion of the ligand also involves a departure from planarity of the double-bond substituents by 5.5°.

Stabilization and Electronic Structure of the Mixed-Valence Complex $[(FeCp^*)_2$(biphenyl)$]^+(PF_6^-)$. In the course of the

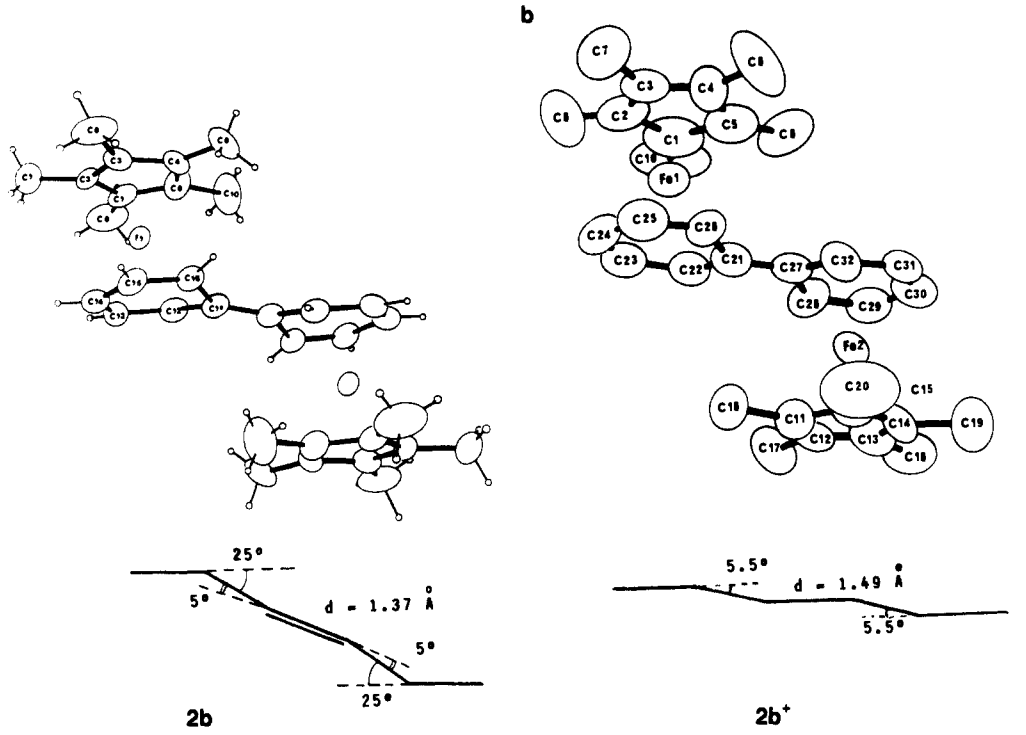

Figure 3. X-ray molecular structure of **2b** and **2b**$^+$.[10a,b] The schemes (bottom) show the distortions of the biphenyl ligands.

Table IV. Mössbauer Data for Organoiron Bisandwiches $[(FeCp^*)_2(biphenyl)]^{n+}$

n	complex	T, K	IS,[a] mm/s	QS,[b] mm/s	Γ,[c] mm/s
		300	0.462 (3)	1.285 (4)	0.28 (1)
2	**2b**$^{2+}$	78	0.568 (1)	1.321 (1)	0.272 (2)
		300	0.498 (1)	1.222 (3)	0.329 (5)[d]
1	**2b**$^+$	78	0.567 (1)	1.249 (2)	0.345 (3)[d]
		300	0.490 (2)	1.653 (7)	0.254 (6)
0	**2b**	78	0.564 (1)	1.653 (2)	0.278 (4)

[a] IS are isomer shift values referred to metallic iron at 300 K. [b] QS are quadrupole splittings. [c] Γ are Lorenzian widths at half-height. [d] Average values over the two lines.

Na/Hg reduction of **2b**$^{2+}$ to **2b**, a transient green color was observed. This encouraged us to attempt a rationale synthesis of the hoped-for mixed-valence complex **2b**$^+$ by comproportionation. Indeed, mixing equimolar amounts of **2b** and **2b**$^{2+}$ in THF at 20 °C gives the air-sensitive but thermally stable green complex **2b**$^+$ in 80% yield after recrystallization from acetone at −40 °C (eq 5).

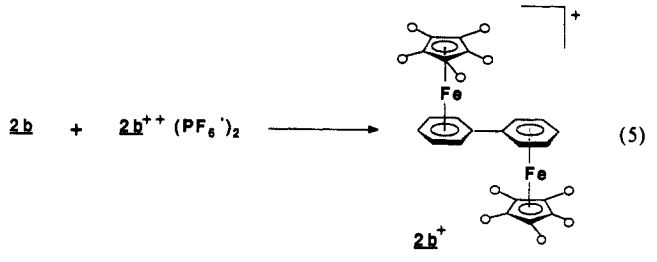

The paramagnetism of **2b**$^+$ is shown by its ESR spectrum in frozen THF at 4 K consisting of three g values characteristic of the rhombic distortion of Fe^I and Fe^IFe^{II} complexes (g_x = 2.0394; g_y = 1.9838; g_z = 1.9378).

The X-ray crystal structure of **2b**$^+$ has been reported in a preliminary communication.[10b] The unit cell contains two independent molecules with similar structures, close to the C_{2h} symmetry. One of these molecules is represented in Figure 3b. They are characterized by an exocyclic interatomic distance consistent with a conjugated single bond (respectively, 1.49 Å for C_{21}–C_{27} and 1.47 Å for the other molecule). Their phenyl ligands are almost flat (folding angle 5.5°), with a coordination to the two iron atoms, which can be viewed as being of distorted η^6 mode with one long bond corresponding to the carbons linking the phenyl rings (average 2.25 Å; range 2.23–2.27 Å), and five shorter bonds (average 2.07 Å; range 1.99–2.16 Å).

The Mössbauer spectrum of the powder at zero field is a doublet and the parameters are intermediate between those of the Fe^I and

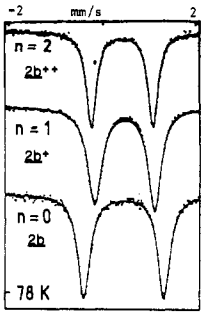

Figure 4. Mössbauer spectra of $[(FeCp)_2(biphenyl)]^{n+}$ (n = 0–2) at zero field and 78 K. **2b**$^{2+}$ (n = 2) behaves as two independent 18e cationic sandwich complexes: **2b**$^+$ (n = 1) is a delocalized 37e complex; **2b** (n = 0) also behaves as two independent 18e natural complexes.

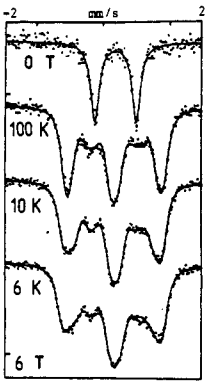

Figure 5. Mössbauer spectra of $[(FeCp^*)_2(biphenyl)]^+PF_6^-$ (**2b**$^+$) under a 6-T longtidinal magnetic field. Notice the thermal dependence due to the paramagnetic effect of the 37th electron. The diamagnetic and neutral complexes do not show thermal dependence in agreement with their diamagnetism.

Fe^{II} sandwich complexes (Table IV and Figure 4). Interestingly, these parameters do not depend on temperature, in contrast to monomeric Jahn–Teller Fe^{I} sandwiches. These trends clearly indicate that $\mathbf{2b}^+$ is an average-valence complex on the Mössbauer time scale. More precisely, $\mathbf{2b}^+$ is either a delocalized mixed-valence complex or the hopping $Fe^{I} \rightleftarrows Fe^{II}$ is faster than the Mössbauer time scale. Investigation of the near-infrared spectra usually allows a distinction between these two situations,[3-5] but experiments have not been successful with the $Fe^{I}Fe^{II}$ series.

The Mössbauer spectra under magnetic field allow determination of the spin density on the metals by measuring the magnetic hyperfine interaction. Measurements under 6 T (Figure 3) show a paramagnetic effect; the hyperfine field created along the three principal axes of the magnetic system (supposed to match the [EFG] axes) can be measured. The data (Table IV) are interpreted in the simple model of a spin $^1/_2$ with $g = 2$.

$$\vec{H}_{hyp} = -[A]\langle S\rangle/S$$

where [A] is a "saturation hyperfine field tensor" and $\langle S\rangle$ a thermal average given by the adequate Brillouin's function:

$$\langle S\rangle = SB_{1/2}(2\mu_B H_{ext}/k_B T)$$

It is worth noting that the $[A]$ tensor determined this way (Table IV) has an isotropic value, −3.3 T, which mainly represents the contact term: indeed with $g_{iso} = 1.987$, the expected orbital contribution

$$(A_L)_{iso} = (g_{iso} - 2)29\ T^{13} = -0.4\ T$$

can be dropped, and on the other hand, the spin-dipolar term is canceled. So, such a low value of the contact term, compared with the expected value for a spin $^1/_2$ (−12.7 T^{13}) shows that each iron atom experiences only 25% of the total unpaired spin density. This value contrasts somewhat with the 40% value found for $\mathbf{1b}^+$.[9d]

Theoretical Study

In order to shed some light on the electrochemical and structural behavior of the studied complexes, we have carried out calculations on compounds $\mathbf{1a}^{2+}$, $\mathbf{2a}^{2+}$, $\mathbf{2a}^+$, and **2a**, using the SCF–MS–Xα method.[14] Indeed, this method has been proven to be particularly useful for the rationalization of the bonding in closed- and open-shell sandwich complexes.[15] In particular, we have recently analyzed by this method the electronic structures of several 18- and 19-electron CpFe(arene) derivatives,[10d] which are of course related to the electronic structure of the $\mathbf{1a}^{2+}$–**2a** dimers. The results obtained for CpFe(benzene)$^+$ and CpFe(benzene)[10d,16] lead to the following level ordering:

$$\pi(\text{benzene}) < \pi(\text{Cp}) < \text{Fe}(x^2-y^2, xy) < \text{Fe}(z^2) << \text{Fe}(xz, yz) < \pi^*(\text{benzene}) < \pi^*(\text{Cp})$$

(the z axis being the pseudocylindrical axis). The pseudodegenerate xz, yz set is vacant in the case of the cation and singly occupied in the case of the 19-electron neutral molecule. Of peculiar importance for the following discussion is the level ordering of the π and π^* ligand levels (only the two doubly degenerate sets of the ligands π systems are considered here). This level ordering is the same for the free ligands and takes its origin from their different topologies.

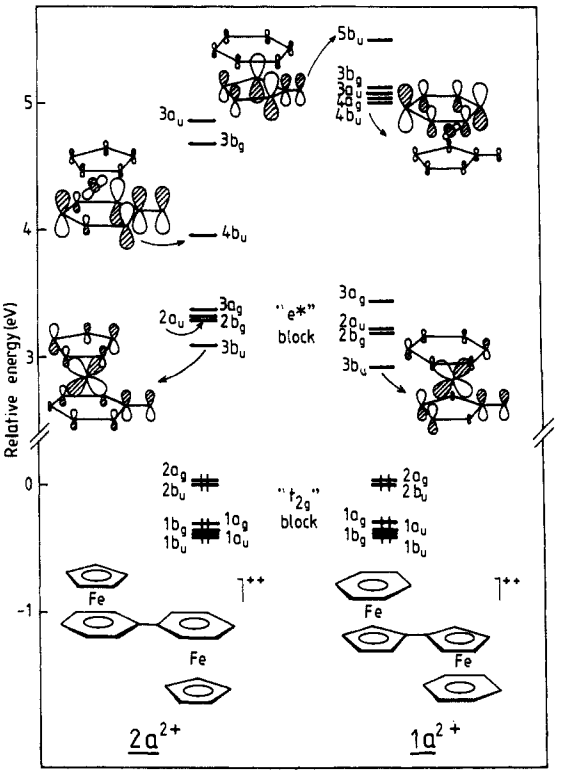

Figure 6. MO-level diagrams of $\mathbf{1a}^{2+}$ and $\mathbf{2a}^{2+}$. The two diagrams have been rescaled by placing their $3d_{z^2}$ nonbonding levels at the same energy.

Table V. Measured Values of the "Hyperfine field" Tensor [A] (Complex $\mathbf{2b}^+$)

T, K	$\langle S\rangle/S$ (calcd)	A_x, T	A_y, T	A_z, T	A_{iso}, T
10	0.199	−10.6	+1.7	−2.1	−3.7
6	0.324	−9.5	+1.9	−1.1	−2.9
av		−10.0	+1.8	−1.6	−3.3

We start our analysis with the two 36-electron isomers $\mathbf{1a}^{2+}$ and $\mathbf{2a}^{2+}$. Our results on $\mathbf{1a}^{2+}$ are in qualitative agreement with previous calculations on this complex.[9d] In this paper we focus the discussion on the similarities and differences between the two isomers. The two compounds can be considered as dimers made from two monomers having the same skeletal MOs as [CpFe(benzene)]$^+$. Each of the monomeric levels generates in the dimers a pair of in-phase and out-of-phase combinations, which are easily identified in Figure 6, which show the energy level diagram calculated for $\mathbf{1a}^{2+}$ and $\mathbf{2a}^{2+}$. Table V indicates the charge distribution in some of these levels. Both dimers exhibit a block of six occupied low-lying levels derived from the monomeric "t_{2g}" set (the x^2-y^2 and xy levels being slightly below z^2 orbitals) lying below a block of four vacant levels of dominant xz and yz ("e*") character. The energy splitting between two in-phase and out-of-phase components is negligible in the t_{2g} block, since these levels, essentially metallic in character, cannot significantly overlap. This splitting is moderate between the xz components (a_g and b_u), which have some minor character on the carbon atoms linking the two monomers. The difference between the two energy diagrams lies in the upper levels, which are of ligand-dominant character. As in CpFe(benzene)$^+$ and, for the same reason, in both $\mathbf{1a}^{2+}$ and $\mathbf{2a}^{2+}$ these levels are derived from the π^*(benzene) orbitals. However, in the case of $\mathbf{2a}^{2+}$, the π^* components of the two phenyl rings, which are symmetrical with respect to the symmetry plane of the molecule, overlap strongly because of their important localization on the carbon atoms linking the two monomers.

(13) Mariot, J. P.; Michaud, M.; Lauer, S.; Astruc, D.; Trautwein, A. X.; Varret, F. *Hyperfine Interact.* **1983**, *14*, 333; *J. Phys.* **1983**, *44*, 1377.
(14) (a) Slater, J. C. *Adv. Quantum Chem.* **1972**, *6*, 1. (b) Johnson, K. H. *Adv. Quantum Chem.* **1973**, *7*, 143.
(15) (a) Weber, J.; Geoffroy, M.; Penigault, A. *J. Am. Chem. Soc.* **1978**, *100*, 3395. (b) Weber, J.; Kundig, E. P.; Goursot, A.; Penigault, A. *Can. J. Chem.* **1985**, *63*, 1734. (c) Osborne, J.-H.; Trogler, W. C.; Morand, P. C.; Francis, C. G. *Organometallics* **1987**, *6*, 94. (d) Rösch, N.; Klemperer, W. G.; Johnson, K. H. *Chem. Phys. Lett.* **1973**, *23*, 149. (e) Case, D. A.; Karplus, M. *J. Am. Chem. Soc.* **1977**, *99*, 6132. (f) Goursot, A.; Penigault, A.; Weber, J. *Nouv. J. Chim.* **1979**, *3*, 675. (g) Case, D. A.; Huyng, B. H.; Karplus, M. *J. Am. Chem. Soc.* **1979**, *101*, 433. (h) Norman, J. G.; Renzoni, G. E.; Case, D. A. *J. Am. Chem. Soc.* **1979**, *101*, 5256. (i) Anderson, J. G.; Fehlner, T. P.; Foti, A. E.; Slahub, D. R. *J. Am. Chem. Soc.* **1980**, *102*, 422. (j) Sunil, K. K.; Rogers, M. T. *Inorg. Chem.* **1981**, *20*, 3233. (k) Weber, J.; Goursot, A.; Penigault, A.; Ammeter, J. H.; Bachman, J. *J. Am. Chem. Soc.* **1982**, *104*, 1491. (l) Perfield, K. W.; Gervith, A. A.; Solomon, E. F. *J. Am. Chem. Soc.* **1985**, *107*, 4519.
(16) (a) Le Beuze, A.; Lissilour, R.; Roch, M.; Weber, J., to be submitted for publication. (b) Le Beuze, A.; Lissilour, R.; Weber, J., to be submitted for publication.

Scheme II: Qualitative π MO Diagram of Biphenyl and Fulvalene, Constructed from the π and π^* Orbitals of Benzene and of the Cyclopentadienyl Anion, Respectively[a]

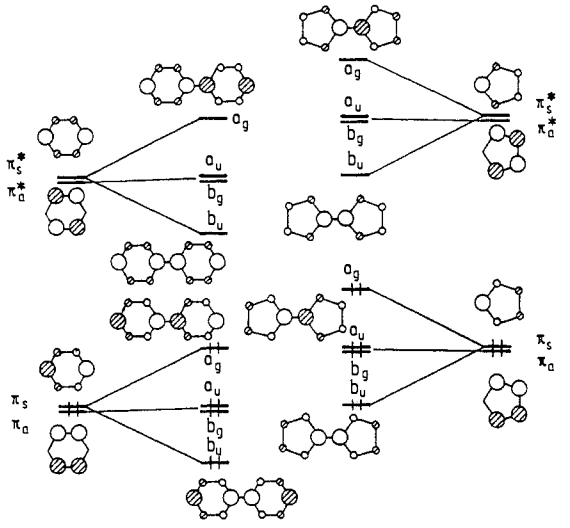

[a] The energy levels of the dimers are labeled with respect to the C_{2h} symmetry.

Therefore, their $4b_u$ bonding combination lies not far above the e* block. The situation is different in $\mathbf{1a}^{2+}$: since the two arenic rings are not bonded, the four levels derived from the π^*(benzene) levels afford no energy splitting and lie at an energy close to the one of the corresponding levels in CpFe(benzene)$^+$. In compound $\mathbf{1a}^{2+}$, the vacant monomeric MOs which overlap are, this time, the symmetrical components of the π^* cyclopentadienylic rings. However, since the π^*(Cp) levels lie at higher energy than their benzenic homologues, their bonding combination ($5b_u$) remains high in energy, above the π^*(benzene) levels. Scheme II illustrates qualitatively the differences between the frontier orbitals of the biphenyl and the fulvalene ligands. As we shall see below, it is the accessibility of the $4b_u$ level upon reduction in $\mathbf{2a}^{2+}$ and its related compounds that makes the difference between the electrochemical behaviors of the biphenylic- and the fulvenic-type dinuclear 36-electron complexes.

The energy level diagrams of complexes $\mathbf{2a}^{2+}$, $\mathbf{2a}^{+}$, and **2a** are shown together in Figure 5. In order to make the results comparable, the two MO diagrams have been adjusted by placing their essentially nonbonding $3d_{z^2}$ levels at the same energy. By using this rescaling procedure, one can avoid the energy shift between the levels of different complexes, which is an artifact of the "muffin tin" approximation. The larger difference observed is between $\mathbf{2a}^{+}$ and **2a**. This is consistent with the geometries used in the calculations (idealized experimental structures): as said previously, the major structural change occurs during the second electron transfer. The $3b_u$ LUMO of $\mathbf{1a}^{2+}$ is the level that accepts one and then two electrons upon reduction. However, as one can see in Table VI, the localization of this level changes drastically when going from $\mathbf{2a}^{2+}$ to $\mathbf{2a}^{+}$ and to **2a**. As said previously, this level in $\mathbf{2a}^{2+}$ is of metallic dominant character with a weak localization on the biphenyl. In **2a** the localization on the metals drops while the localization on the biphenyl ligand increases at the same time. In particular, the localization of the $3b_u$ level on the pair of C atoms linking the two phenyl rings varies significantly: from 9% to 19% when going from $\mathbf{2a}^{2+}$ to **2a**. The opposite variation is observed for the $4b_u$ level. Clearly, when going from $\mathbf{2a}^{2+}$ to **2a** an avoided level crossing occurs between the $3b_u$ and $4b_u$ levels, i.e., the structural change accompanying the reduction stabilizes the bonding combination of the π^* phenylic orbitals so that it can be occupied by the incoming electrons, inducing a shortening of the C(phenyl)–C(phenyl) bond. The change in the nature of both $3b_u$ and $4b_u$ is nicely illustrated by their plots in $\mathbf{2a}^{2+}$, $\mathbf{2a}^{+}$, and **2a** shown in Figure 7.

The $3b_u$ level in **2a** still has a significant metallic localization, i.e., the mixing of the e* component of b_u symmetry into the ligand

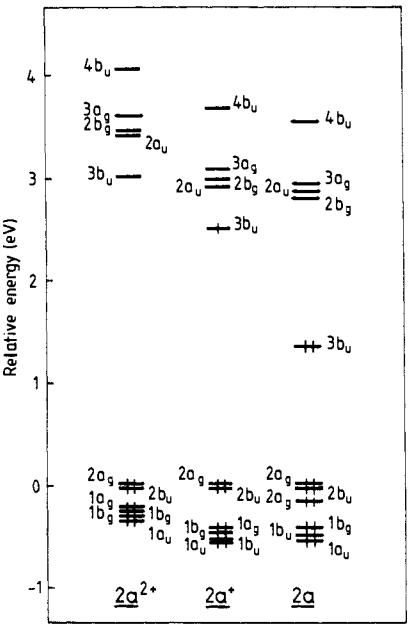

Figure 7. MO-level diagrams of $\mathbf{2a}^{2+}$, $\mathbf{2a}^{+}$, and **2a**. The three diagrams have been rescaled by placing their $3d_{z^2}$ nonbonding levels at the same energy.

π^* b_u level is still large in **2a**. Such a situation is, at first sight, surprising since, in **2a**, the C(phenyl)–C(phenyl) bond distance, 1.37 Å, corresponds unambiguously to a full double bond. Clearly, other MO levels have to be considered. Indeed, the formation of a bond can be induced by both occupation of a bonding orbital and/or unoccupation of antibonding orbitals. Then the C(phenyl)–C(phenyl) antibonding orbital that one has to check is the highest occupied level of biphenyl shown on Scheme II, of a_g symmetry, which is an antibonding combination of the π_s bonding phenylic levels. If one wants to identify this orbital in the calculated MO diagram of $\mathbf{2a}^{2+}$, one finds a level lying $\approx$0.5 eV below the t_{2g} block, which has an overall 11% localization on the two C atoms linking the two phenyl rings. This localization drops to 10% and then to 5% when going to $\mathbf{2a}^{+}$ and **2a**. In fact, because of their proximity in energy, all the highest occupied a_g levels mix somewhat together and, consequently, get some localization on the above-mentioned C atoms. When going from $\mathbf{2a}^{2+}$ to **2a** the block of the highest occupied a_g levels loses 0.3 electron on this pair of carbon atoms. This weakening of π_{CC} antibonding character of the occupied a_g levels upon reduction arises from the shifting up in energy of the occupied a_g MO of Scheme II when the C–C bond is shortened. This destabilization allows this level to mix with vacant a_g levels in the complex, in a way that tends to balance the destabilization, i.e., in reducing its π_{CC} antibonding character. Obviously, this loss of antibonding character by the occupied a_g levels upon reduction brings a secondary but significant contribution to the building of the C(phenyl)–C(phenyl) double bond in **2a**.

Going back to the comparison of the accessibilities of the vacant MOs in compounds $\mathbf{1a}^{2+}$ and $\mathbf{2a}^{2+}$, it is now clear that, because of the high energy of its $4b_u$ level, no structural reorganization of the fulvalene ligand upon reduction is expected for $\mathbf{1a}^{2+}$ and related compounds. In fact, the only ligand levels of $\mathbf{1a}^{2+}$ that appear accessible upon reduction are the π^*(benzene) orbitals (see Figure 5). Therefore the reduction of $\mathbf{1a}^{2+}$ is expected to populate levels that are essentially metallic in character and/or π^*(benzene) levels, the former being more accessible than the latter. Cyclic voltammetry experiments on $[Fe_2(arene)_2(fulvalene)]^{2+}$ dimers are fully consistent with these MO arguments since it has been shown that the first three transferred electrons affect the iron oxidation states (successively $Fe^{II}Fe^{I}$, $Fe^{I}Fe^{I}$, $Fe^{I}Fe^{0}$), while the transfer of a fourth electron presumably induces a structural reorganization, which could be an η^6 to η^4 hapticity change of the metal atoms, associated with a formal 2-electron reduction of the arene rings.[9d]

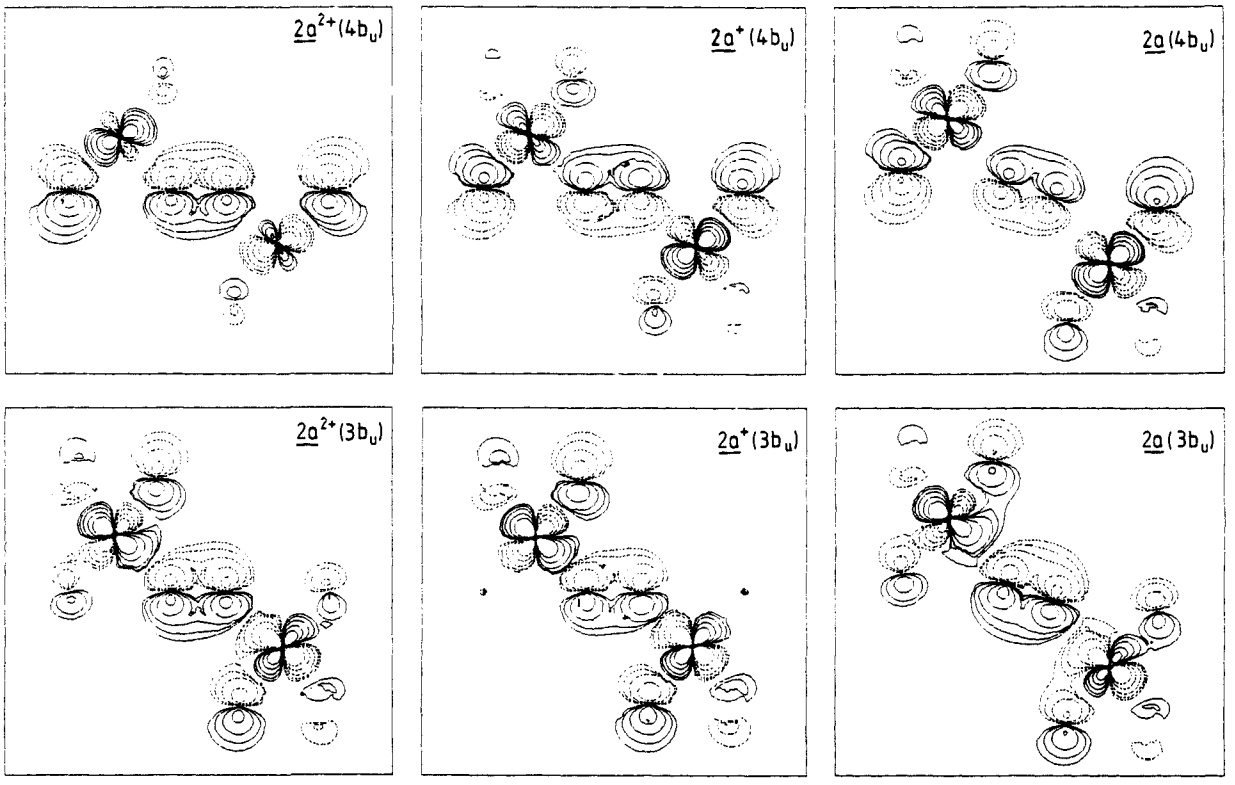

Figure 8. Contour plots in the symmetry plane of the molecule of the $3b_u$ and $4b_u$ MO in $\mathbf{2a}^{2+}$, $\mathbf{2a}^{+}$, and **2a**.

Discussion

The two-electron transfer found in the reduction of the parent complex $\mathbf{2a}^{2+}$ to **2a** is decomposed in two one-electron reductions $\mathbf{2b}^{2+} \rightarrow \mathbf{2b}^{+}$ and $\mathbf{2b}^{+} \rightarrow \mathbf{2b}$ when the Cp ligand is permethylated (Cp*). The deep blue color, absence of ESR spectrum, and two-electron step indicate that the same structural rearrangement from a biphenyl complex $\mathbf{2}^{2+}$ to a bicyclohexadienylidene complex **2** occurs in both the Cp and Cp* series upon bielectronic reduction. However, the Cp* series offers a unique opportunity to disclose the structural rearrangement concomitant with each electron transfer since the X-ray structures of both the one-electron reduction product $\mathbf{2b}^{+}$ and the two-electron reduction product **2b** are available. Two hypotheses could formally account for a structural rearrangement in a fast two-electron transfer. The first one implies that the structural rearrangement (SR) intervenes concomitant with the first electron transer (i), and the second one involves a structural rearrangement concomitant with the second electron transfer (ii). In the case of a 36-electron precursor, these two hypotheses can be summarized as follows in terms of valence electron count:

$$36e \xrightarrow[SR]{e} 35e \xrightarrow{e} 36e \qquad \text{(i)}$$

$$36e \xrightarrow{e} 37e \xrightarrow[SR]{e} 36e \qquad \text{(ii)}$$

The X-ray crystal structure of $\mathbf{2b}^{+}$ shows an almost completely planar biphenyl ring and the Mössbauer spectra indicate a delocalized mixed valence (fast e hopping) or average-valence complex. Thus, $\mathbf{2b}^{+}$ is a 37-electron complex with almost no structural change as compared to the precursor 36e complex. On the other hand, the X-ray crystal structure of **2b** shows a considerable structural change with a bicyclohexadienylidene ligand. This is corroborated by the NMR and Mössbauer data showing that **2b** is diamagnetic, unlike **1b**, which is a biradical. The complex **2b** can be assigned a 36e state, each half of the bicyclohexadienylidene ligand being bound to an iron atom in a η^5-cyclohexadienyl-like mode. Thus, the structural rearrangement occurs essentially concomitant with the second electron transfer (fast electrochemical kinetics).[10a,b] The difference in energy between the structure found for **2b** and that of a 38e biradical, which would still contain an undistorted biphenyl ligand, corresponds to a stabilization. This energy gain makes the second electron-transfer step less difficult and thus shifts the second reduction potential toward a less negative value. In the Cp series, this energy gain obtained upon structural reorganization concomitant with the second electron transfer fully compensates the additional electrostatic repulsion so that both electrons are transferred in a single step. This is fortunately not quite the case in the Cp* series, which allowed isolating $\mathbf{2b}^{+}$. However, the two electron transfers are still energetically close so that the comproportionation constant is not very large: $K = 172$ at 20 °C. Thus, these thermodynamic data deduced from the values of the thermodynamic potentials of $\mathbf{2a}^{2+}$ and $\mathbf{2b}^{2+}$ can be compared to those of $\mathbf{1a}^{2+}$ and $\mathbf{1b}^{2+}$. The bielectronic reductions of $\mathbf{1a}^{2+}$ and $\mathbf{1b}^{2+}$ can serve as references since no significant structural reorganization occurs upon reduction. Since the two first reduction waves of $\mathbf{1a}^{2+}$, isomer of $\mathbf{1a}^{2+}$, are separated by $\Delta E° = 0.32$ V, the reorganization energy of

$$[(Fe^{I}Cp^{*})_2(\text{biphenyl})] \rightarrow [(Fe^{II}Cp^{*})_2(\text{bicyclohexadienylidene})]$$

in **2b** can be estimated to be of the same order e.g., using Weller's equation:[17a,b]

$$\Delta G° = \Delta E° \times 23 = -7.4 \text{ kcal mol}^{-1} = -30.9 \text{ kJ mol}^{-1}$$

Similarly, in the permethylated series, this reorganization energy can be best estimated by comparison of the difference between the $E°$ values of the two waves of $\mathbf{1b}^{2+}$ ($\Delta E°_1 = 0.48$ V) and $\mathbf{2b}^{2+}$ ($\Delta E°_2 = 0.13$ V):

$$\Delta G° = (\Delta E°_2 - \Delta E°_1) \times 23 = -8.1 \text{ kcal mol}^{-1} = -33.9 \text{ kJ mol}^{-1}$$

Another reference complex is {biphenyl[$Cr(CO)_3$]$_2$}, which was shown by Rieke[17c-e] to also be reduced in a single two-electron

(17) (a) Rehm, D.; Weller, A. *Isr. J. Chem.* **1970**, *16*, 259. (b) Weller, A. *Pure Appl. Chem.* **1968**, *16*, 115. (c) Rieke, R. D.; Henry, W. P.; Arney, J. S. *Inorg. Chem.* **1987**, *26*, 420. (d) Milligan, S. N.; Rieke, R. D. *Organometallics* **1983**, *2*, 171. (e) Rieke, R. D.; Milligan, S. N. *Organometallics* **1987**, *6*, 699.

step as $2a^{2+}$. Rieke[17e] could also recently show by NMR that the biphenyl ligand of the dianion adopts a bicyclohexadienylidene structure. The NMR data for this ligand are very close to **2b** and $\{biphenyl[Cr(CO)_3]_2\}^{2-}$. In the absence of structural information for the thermodynamically unstable mixed-valence anion, Rieke proposed the other hypothesis (i), e.g., structural reorganization occurring concomitant with the first electron transfer. The great similarity between the behaviors of the chromium and iron systems (a single two-electron wave and rearrangement from biphenyl to bicyclohexadienylidene upon two-electron reduction) indicates that the structural reorganization presumably also occurs concomitant with the second electron transfer in the chromium case, e.g., hypothesis ii.

Three monometallic series of transition-metal–arene complexes also show a two-electron transfer[18] with η^6 to η^4 decoordination: $Ru(arene)_2^{2+}$, $MCp^*(C_6Me_6)$, M = Rh or Ir and $Cr(arene)L_3$, L_3 = arene or $(CO)_3$. Recent spectroscopic data[18e] favor a structural rearrangement in the course of the second electron-transfer step in the Rh complex but no X-ray crystal structure is available for any single electron-transfer intermediate. On the other hand, with $Cr(arene)L_3$, L_3 = arene or $(CO)_3$, it was proposed that the partial decoordination occurs after the first electron transfer.[18f,g]

Conclusions

The synthesis and stabilization by permethylation of Cp ligand of the novel sets of complexes 2^{n+} (n = 0–2) leads to the first case for which a 2e transfer involving a structural rearrangement (Cp series) can be decomposed into two close, but structurally and electronically characterized, ET steps (Cp* series).

This accurate structural and electronic information indicates that the structural rearrangement arises essentially concomitant with the second ET. The arene-linked series compares with the isomeric Cp-linked series that does not rearrange upon a 2e transfer, the difference being taken into account by the existence, in the biphenyl series only, of a low-lying unoccupied b_u MO localized on the two coupled rings.

The addition of one electron in the b_u LUMO level provokes only a slight distortion of the biphenyl ligand (5.5° folding) so that the 37e complex $\mathbf{1b}^+$ also has a μ_2,η^{12}-biphenyl ligand. On the other hand, the parent binuclear radical $\mathbf{1a}^+$ is not thermodynamically stable. The unicity of the Mössbauer doublet, at zero field, shows that $\mathbf{1b}^+$ is an average-valence complex on the Mössbauer time scale of 10^{-8} s^{-1} (delocalization or fast hopping). The spectra under 6 T show that about half of the spin density is located on the two iron atoms, in agreement with our calculations, which also indicates that the majority of the other half is on the biphenyl ligand, explaining the slight distortion of the latter.

The addition of the second electron in the b_u HOMO induces a deep stereoelectronic rearrangement of the biphenyl ligand since the folding is now of 25° and the inter-ring distance of 1.37 Å is that of a double bond. The ^1H and ^{13}C NMR spectra, the absence of ESR spectra, and the Mössbauer spectra all show the diamagnetism, e.g., the intramolecular chemical coupling of **1a** (isomer of the biradical **2a**) and of **1b** (Scheme I).

The energy of the stereoelectronic rearrangement $[(Fe^ICp)_2(biphenyl)] \rightarrow [(Fe^{II}Cp)_2(bicyclohexadienylidene)]$ occurring during the second ET can be estimated by comparison with the isomer $[Fe^{II}_2(fulvalene)(C_6H_6)_2]$, which does not rearrange. A fundamental principle derived thereof is that a fast two-electron transfer occurs when this reorganization energy (here 32–34 KJ mol^{-1}) fully compensates the electrostatic factor which would separate the reduction potential of a dication from that of a monocation in the absence of rearrangement.

Experimental Section

(1) General Data. All manipulations of sensitive materials were conducted in a VAC argon drybox or under argon in a Schlenk apparatus connected to a double manifold providing vacuum and dry argon. Reagent-grade tetrahydrofuran, pentane, and toluene were predried on Na foil and distilled from sodium benzophenone ketyl under argon. All other chemicals were used as received. ^1H NMR spectra were obtained with a Brucker AC 200 spectrometer and the ^{13}C NMR spectra were recorded with a Brucker AC 200 (50.3 MHz) or a Brucker (67.9 MHz). NMR spectra were referenced to Me_4Si (^1H) or the appropriate deuterated solvent (^{13}C). Elemental analyses were performed by the CNRS Center of Microanalyses at Lyon-Villeurbanne.

(2) Electrochemistry. Cyclic voltametry data were recorded with a PAR 273 potentiostat galvanostat. The effect of solution resistance was minimized by the use of positive feedback compensation and dilute solutions (10^{-4} mol L^{-1}) to keep currents around 1–2 μA. Thermodynamic potentials were recorded with reference to an aqueous SCE segregated from the test solution by a fine frit containing a DMF solution (n-Bu_4NBF_4, 0.1 M). The electrode material (Hg or Pt cathode) was not found to influence the $E°$ values. The switching potential E_{sp} was chosen far enough away from the peak potential (at least 150 mV) so that its effect remained small. DMF was preferred to MeCN because of the lack of chemical reversibility of the wave with the latter solvent. Diffusion-controlled electron transfers were systematically checked by verifying that i_{pc} $V^{-1/2}$ was constant over a wide scan range. The thermodynamic potentials values $E°$ reported in Table I were obtained by taking the average of E_{pa} and E_{pc} since the waves were reversible. The number of electrons for each reversible wave was determined by comparison with the height the wave of oxidation of ferrocene (independently we checked that ferrocene and biferrocene showed comparable heights of the monooxidation waves). In the Cp* series of biphenyl complexes, the two-electron reductions were checked by determination of the molecular and X-ray structures of the reduction products.[10a,b]

(3) $[Fe_2(biphenyl)Cp_2]^{2+}(PF_6^-)_2$ ($2a^{2+}$). The reaction was carried out in a 250-mL three-necked round-bottomed flask equipped with a nitrogen inlet and a reflux condenser topped with a gas outlet. A mixture of 18.6 g (100 mmol) of ferrocene, 13.3 g (100 mmol) of $AlCl_3$, 0.54 g (20 mmol) of Al powder, and 1.5 g (10 mmol) of biphenyl was stirred for 5 min under argon. The mixture was heated in the melt to 120 °C under argon and with agitation, for 16 h with an oil bath. The reaction mixture was hydrolyzed slowly with 100 mL of degassed ice/water and addition of concentrated NH_4OH until pH 9 precipitated $Al(OH)_3$. After filtration, a yellow solid was obtained by addition of an aqueous HPF_6 (10 mmol) solution. The precipitate was filtered, dissolved in 50 mL of acetonitrile, and dried for 1 h over $MgSO_4$. After filtration through a 2-cm layer of Al_2O_3, addition of 20 mL of ethanol to the yellow solution followed by slow evaporation of the acetonitrile using a rotary evaporator, gave yellow microcrystals of $2a^{2+}$, 3.6 g (53.4% yield), found to be pure by ^1H NMR.

(4) $[Fe_2(p,p'$-dimethylbiphenyl$)Cp_2]^{2+}(PF_6^-)_2$ ($2c^{2+}$). **Procedure 3**, applied to 0.2 g (1.1 mmol) of p,p'-dimethylbiphenyl, 2 g (11 mmol) of ferrocene, 2 g (15 mmol) of $AlCl_3$, and 0.1 g (3 mmol) of Al powder at 120 °C, provided 0.410 g (52% yield) of yellow microcrystals of $2c^{2+}$. Anal. Calcd. for $C_{24}H_{24}P_2F_{12}$: C, 40.34; H, 3.36. Found C, 40.40; H, 3.35. ^1H NMR (CD_3CN, TMS) δ 6.5 (m, aromatic CH, 8 H), 4.86 (s, C_5H_5, 10 H), 2.5 (s, CH_3, 6 H).

(5) $[Fe_2(biphenyl)Cp^*_2]^{2+}(PF_6^-)_2$ ($2b^{2+}$). The reaction was carried out as in **3**: $FeCp^*(CO)_2Br$ (9.8 g, 30 mmol), $AlCl_3$ (27 g, 200 mmol), and biphenyl (0.8, 5 mmol) were stirred for 5 min under argon. The mixture was heated in the melt to 120 °C under argon with agitation for 2 days with an oil bath. While still in the melt, the reaction mixture was hydrolyzed very slowly with 200 mL of degassed ice/water. Addition of concentrated NH_4OH was continued until pH 9 precipitated $Al(OH)_3$. After filtration, a yellow solid was obtained by addition of an aqueous HPF_6 (10 mmol) solution. The precipitate was filtered, dissolved in 50 mL of acetonitrile and dried for 1 h over $MgSO_4$. After filtration through a 2-cm layer of Al_2O_3, addition of 20 mL of ethanol to the yellow solution, followed by slow evaporation of the acetonitrile under reduced pressure, gave 1.36 g (32% yield) of yellow microcrystals of $2b^{2+}$. Anal.

(18) (a) Laganis, E. D.; Voegeli, R. H.; Swarin, R. T.; Finke, R. G.; Voegeli, R. H.; Loganis, E. D.; Boekelheide, V. *Organometallics* **1983**, *2*, 347. (b) Lockemeyer, J. R.; Rauchfuss, T. B.; Rheingold, A. L.; Wilson, S. R. *J. Am. Chem. Soc.* **1989**, *111*, 8828. (c) Hee, C. K.; Hanson, A. W.; Boekelheide, V. *J. Am. Chem. Soc.* **1985**, *107*, 1979. (d) Bowyer, W. J.; Geiger, W. E. *J. Am. Chem. Soc.* **1985**, *107*, 5657. Pierce, D. T.; Geiger, W. E. *J. Am. Chem. Soc.* **1989**, *111*, 7636. Bowyer, W. J.; Merkert, J. W.; Geiger, W. E.; Rheingold, A. L. *Organometallics* **1989**, *8*, 191. Ogivy, A. F.; Rauchfuss, T. B. *Organometallics* **1989**, *8*, 2739. (e) Merkert, J.; Nielson, R. M.; Weaver, M. J.; Geiger, W. E. *J. Am. Chem. Soc.* **1989**, *111*, 7084. (f) Leong, V. S.; Cooper, N. J. *J. Am. Chem. Soc.* **1988**, *110*, 2645. (g) Elschenbroich, C.; Bilger, E.; Koch, J.; Weber, J. *J. Am. Chem. Soc.* **1984**, *106*, 4297. (h) Plitzko, K.-D.; Rapko, B.; Gollas, B.; Wehrle, G.; Weakley, T.; Pierce, D. T.; Geiger, W. E.; Haddon, R. C.; Boekelheide, V. *J. Am. Chem. Soc.* **1990**, *112*, 6545. Plitzko, K.-D.; Wehrle, G.; Gollas, B.; Rapko, B.; Dannheim, J.; Boekelheide, V. *J. Am. Chem. Soc.* **1990**, *112*, 6556.

(19) (a) Varret, F. *J. Phys. Chem. Solids* **1976**, *37*, 257. (b) Mariot, J. P.; Guillin, J.; Varret, F. *Hyperfine Interact.* **1986**, *30*, 221.

Table VI. Charge Distribution in the Crucial MO Levels of $\mathbf{1a}^{2+}$, $\mathbf{2a}^{2+}$, $\mathbf{2a}^{+}$, and **2a**

localization, %	$\mathbf{1a}^{2+}$					$\mathbf{2a}^{2+}$					$\mathbf{2a}^{+}$					**2a**				
	Fe	Cp	L[a]	i[b]	o[b]	Fe	Cp	L[a]	i[b]	o[b]	Fe	Cp	L[a]	i[b]	o[b]	Fe	Cp	L[a]	i[b]	o[a]
$3b_u$	59	17	12	11	1	50	22	14	14	0	42	16	25	17	0	37	12	33	18	0
$2b_g$	55	21	11	13	0	53	24	09	13	1	53	20	12	15	0	57	18	11	14	0
$2a_u$	54	22	11	13	0	52	23	10	15	0	53	20	12	14	1	57	18	11	13	1
$3a_g$	50	28	10	12	0	52	22	12	13	1	54	20	12	14	0	54	17	15	14	0
$4b_u(5b_u^c)$	4	53	01	41	1	16	03	59	22	0	27	07	45	20	1	37	10	34	18	1

[a] $1a^{++}$: L = C_6H_6; $2a^{++}$, $2a^{+}$ and $2a$: L = $C_{12}H_{10}$. [b] i = inner sphere; o = outer sphere. [c] In the case of $1a^{++}$.

Table VII. SCF-MS-Xα Parameters

atomic sphere	radius, au	α
Fe	2.2795	0.711 51
C	1.6535	0.753 31
H	0.8753	0.777 25
E[a] Cp (C_5 ring)	1.0843	0.762 54[c]
E[a] arene (C_6 ring)	1.3226	0.762 54[c]
out[b]	11.6331	0.762 54[c]

[a] Empty sphere. [b] Outer sphere. [c] Weighted average of atomic values.

Calcd. for $C_{32}H_{40}P_2F_{12}Fe_2$: C, 46.48; H, 4.84. Found: C, 46.39; H, 4.83. ^{1}H NMR (CD_3CN, Me_4Si) δ 6.2–6.1 (m, C_6H_5, 10 H), 1.66 (s, C_5Me_5, 30 H); ^{13}C NMR (CD_3CN) δ 95.7 (C of C_6H_5), 93.7 (C of C_5Me_5), 92.6 (CH para), 91.5 (CH meta), 85.8 (CH ortho), 10.1 (CH_3). Mössbauer data (mm/s vs α-Fe at room temperature, 298 K) IS 0.462, QS 1.285.

(6) [Fe$_2$(*p*,*p*'-dimethylbiphenyl)Cp*$_2$]$^{2+}$ ($\mathbf{2d}^{2+}$). Procedure 5, applied to 0.8 g (5 mmol) of *p*,*p*'-dimethylbiphenyl, 9.8 g (30 mmol) of $FeCp^*(CO)_2Br$, and 27 g (200 mmol) of $AlCl_3$ at 120 °C for 2 days, provided 2.2 g (58% yield) of yellow microcrystals of $\mathbf{2d}^{2+}$. Anal. Calcd. for $C_{34}H_{44}P_2F_{12}$: C, 47.77; H, 5.15. Found C, 47.41; H, 5.10. ^{1}H NMR (CD_3CN, TMS) δ 6.06 (m, aromatic CH, 8 H), 2.40 (s, CH_3, 6 H), 1.56 (s, C_5Me_5, 30 H); ^{13}C NMR (CD_3CN, THF) δ 105.8, 94.70 (complexed aromatic C), 92.70 (C of C_5Me_5).

(7) Fe$_2$(μ_2,η^{10}-bicyclohexadienylidene)Cp*$_2$ (2b). A 0.83-g (1 mmol) sample of the dication $\mathbf{2b}^{2+}$ and 50 g (10 mmol) of 1% Na/Hg were stirred for 3 h under argon in 50 mL of THF at room temperature in a Schlenk tube. Then, the blue solution was transferred into another Schlenk tube to remove the Na/Hg. After the THF was removed in vacuo, the dark residue was extracted with a minimum (10 mL) of toluene and filtered by the Schlenk technique. Pentane (100 mL) was added and the solution was cooled to −90 °C, which provided, after rapid filtration, 0.34 g (64% yield) of a dark blue microcrystalline powder of **2b**, very air-sensitive and thermally stable at 20 °C. ^{1}H NMR (C_6D_6) δ 5.6 (m, CH para, 2 H), 4.1 (m, CH meta, 4 H), 2.6 (m, CH ortho, 4 H), 1.8 (s, C_5Me_5, 30 H); ^{13}C NMR (C_6D_6) δ 102.7 (C=C), 85.1 (C of C_5Me_5), 81.9 (CH meta), 77.7 (CH para), 53.1 (CH ortho), 10.8 (CH_3). These attributions were based on ^{1}H and ^{13}C (ortho, meta and para H's); Mössbauer data (mm/s vs α-Fe at room temprature, (298 K) IS 0.49, QS 1.65; (at 78 K) IS 0.56, QS 1.65.

(8) [Fe$_2$(biphenyl)Cp*$_2$]$^+$PF$_6^-$ ($\mathbf{2b}^+$). A THF solution of 0.268 g (0.5 mmol) of the blue neutral complex **2b** was added under argon to a suspension (0.413 g, 0.5 mmol) of the yellow dicationic complex $\mathbf{2b}^{2+}$ in THF. After being stirred for 30 min at room temperature, the solution became colorless and the mixture contained a suspension of a dark green powder. Filtration under argon gave 0.62 g (90% yield) of a dark green powder of $\mathbf{2b}^+$. Anal. Calcd. for $C_{32}H_{40}Fe_2PF_6$: C, 56.39; H, 5.87. Found: C, 56.14; H, 5.85. Mössbauer data (mm/s vs α-Fe at room temperature, 298 K) IS 0.57, QS 1.25; (4.2 K) IS 0.49, QS 1.22. ESR (at 77 K, frozen THF solution) g_x = 2.0458, g_y = 2.0001, g_z = 1.8404.

(9) Mössbauer Data. Mössbauer spectra were recorded with a 25 mCi ^{57}Co source on Rh. The Mössbauer spectrometer operates in the constant acceleration mode; typically, reliability of the velocity scale is 0.2% and IS reproducibility is 0.002 mm/s. The instrumental line width is 0.215 mm/s. The spectra of polycrystalline samples under external field (parallel to the *g* beam) have been stimulated, accounting for an "induced hyperfine field tensor" whose (following ref 19) main components can be fitted and represent the various values the hyperfine field would take if the external field were applied along each of the principal axes of the hyperfine tensor [**A**]; here it has been assumed (contrary to ref 19b) that all involved tensors ([**A**], [$\mathbf{X}_m$], [**EFG**]) have same principal axes.

(10) Computational Details. All the calculations have been carried out within the standard SCF-MS-Xα method.[14] The muffin tin atomic sphere radii used in all the calculations are given in Table VI. They were determined by assuming at first touching spheres in $\mathbf{2a}^{2+}$ and then enlarging the carbon radii by 25% in order to assume a better description of the ring system.[20] An additional empty sphere has been located in the center of each ring. The atomic exchange parameter α was obtained from Schwarz tabulation[21] except for hydrogen, where the Slater value[22] was chosen. Those relative to the extramolecular (outer-sphere) and the inner-sphere regions are weighted-average values to the atomic ones. Potential waves up to l = 2 are included in the multiple scattering expansions in the metal sphere and the extramolecular regions; up to l = 1 in the carbon and empty spheres. Only the l = 0 values was considered for hydrogen spheres. SCF calculations were converged to better than ±0.0001 R_y on each level. The geometries used in the calculations on $\mathbf{2a}^+$ and **2a** are averaged crystal structures of $\mathbf{2b}^+$[10c] and **2b**,[10a] idealized to the C_{2h} symmetry. The structure assumed for the $\mathbf{1a}^{2+}$ and $\mathbf{2a}^{2+}$ dimers is the same as the one used in previous calculations on the FeCp(benzene) monomer,[10b] assuming as a C–C bond distance of 1.50 Å between the two sandwich units. In all the calculations, a C–H distance of 1.10 Å was assumed.[24]

Acknowledgment. We thank the CNRS, the Universities of Bordeause I and Rennes I, and the Region Aquitane for financial support and the "Ministère de la Recherche de la Technologie" for a thesis grant to M.L.

(20) Herman, F.; Williams, A. R.; Johnson, K. H. *J. Chem. Phys.* **1974**, *61*, 3508.
(21) (a) Schwartz, K. *Phys. Rev.* **1972**, *B5*, 2466. (b) Slater, J. C. *Int. J. Quantum Chem.* **1973**, *75*, 533.
(22) Gilmore, C. J. *J. Appl. Crystallogr.* **1984**, *17*, 42.
(23) Richardson, D. E.; Taube, H. *Inorg. Chem.* **1981**, *20*, 1278. *J. Am. Chem. Soc.* **1983**, *105*, 40.
(24) Organometallic Electron Reservoirs. 42. For part 41, see: Mandon, D.; Astruc, D. *Organometallics* **1990**, *9*, 341. For part 40, see: Reference 10d.